Generalized magnetic susceptibilities in metals: Application of the analytic tetrahedron linear energy method to Sc†

J. Rath
Magnetic Theory Group, Physics Department, Northwestern University, Evanston, Illinois 60201

A. J. Freeman
Physics Department, Northwestern University, Evanston, Illinois 60201
and Argonne National Laboratory, Argonne, Illinois 60439

(Received 4 September 1974)

A detailed study of the generalized susceptibility $\chi(\vec{q})$ of Sc metal determined from an accurate augmented-plane-wave method calculation of its energy-band structure is presented. The calculations were done by means of a computational scheme for $\chi(\vec{q})$ derived as an extension of the work of Jepsen and Andersen and Lehmann and Taut on the density-of-states problem. The procedure yields simple *analytic* expressions for the $\chi(\vec{q})$ integral inside a tetrahedral microzone of the Brillouin zone which depends only on the volume of the tetrahedron and the diffrences of the energies at its corners. Constant-matrix-element results have been obtained for Sc which show very good agreement with the results of Liu, Gupta, and Sinha (but with one less peak) and exhibit a first maximum in $\chi(\vec{q})$ at $(0, 0, 0.31)2\pi/c$ [vs $(0, 0, 0.35)2\pi/c$ obtained by Liu *et al.*] which relates very well to dilute rare-earth alloy magnetic ordering at $\vec{q}_m = (0, 0, 0.28)2\pi/c$ and to the kink in the LA-phonon dispersion curve at $(0, 0, 0.27)2\pi/c$.

I. INTRODUCTION

The energy-band method has had great success in providing accurate eigenvalues and hence energy-related results in reasonable agreement with experiment. However, for many experimental quantities, a theoretical evaluation of phase-space integrals (i.e., integrations of some observable operator over the k space of a Brillouin zone) is required to high accuracy. These k-space integrals range from simple density-of-states functions to generalized magnetic susceptibilities, dielectric functions, photoemission energy distributions, etc. For these reasons, a variety of approaches has been formulated, all of which are designed to simplify the problem of the calculations of matrix elements of observable operators over the Brillouin zone (BZ).[1–12] Whereas much of the early work was directed at the problem of accurate determination of the electronic (and phonon) density of states, extensive efforts have been directed recently towards problems such as the accurate calculation of the generalized magnetic susceptibility $\chi(\vec{q})$ which (in the approximation of linear-response theory[13]) gives the response of the magnetization of the electron gas in a metal to a spatially varying field of wave vector $\vec{q}$. Information about structure in $\chi(\vec{q})$ has been related to the magnetic interaction energy of a real metal and hence to the possibility of magnetic ordering with wave vector $\vec{Q}$ and to phonon soft modes and Peierls instabilities.[14] Similarly, observed magnon dispersion may also be related (in a constant-matrix-element approximation) to $\chi(\vec{q})$. For real transition or rare-earth metals, recent efforts have focused on including the actual band structure into the calculations and relating maxima in $\chi(\vec{q})$ to certain nesting features in the Fermi surface. The calculations of Evenson and Liu,[15] Gupta and Sinha,[16] and Liu, Gupta, and Sinha[17] have emphasized the need to include matrix elements in addition to the realistic energy eigenvalues.[18]

A basic problem, however, for any of these studies has been the need for a highly accurate, rapid, and efficient computational method. The main schemes which have been proposed towards performing the required k-space integrations include[1]: (i) the root-sampling method,[10] (ii) the linear discrete methods,[11] (iii) the linear analytic method,[2] (iv) the QUAD scheme,[7] and (v) the hybrid method,[12] and variations of these procedures.[12,19]

Both the accuracy and efficiency of some of these schemes have been discussed in detail by Gilat and Raubenheimer[2] (GR) and by Mueller *et al.*[7] Central to all these methods is (a) the *division* of the irreducible wedge of the BZ into microzones (such as cubes in cubic crystals), (b) some *approximation to the behavior of the energy eigenvalue* [say $E_n(\vec{k})$ of the nth band] throughout the microzone [e.g., in the GR method this energy structure is approximated by a linear function whereas the QUAD scheme expands $E_n(k)$ to full quadratic order in some part of the irreducible wedge], and finally (c) an *integration procedure* (e.g., analytic or Monte Carlo) to carry out the k-space integration.

A major advance in the accurate calculation of densities of states was made independently by Jepsen and Andersen[4] and by Lehmann *et al.*[3] with the introduction of tetrahedrons into the GR method

(rather than the usual cubes). Just as was done by Lipton and Jacobs[5] (for the calculation of the spin susceptibility) who employed values of $E_n(\vec{k})$ at the corners of the cube, Lehmann *et al.*[3] and Jepsen and Andersen[4] showed that the coefficients of the linear-interpolation expression in a tetrahedron are determined uniquely by the values of $E_n(\vec{k})$ at the corners of the tetrahedron and that accurate values of the contribution to the density of states from a tetrahedron could be determined *analytically*.

We present here a detailed study of the generalized susceptibility $\chi(\vec{q})$ of Sc metal determined from an accurate augmented-plane-wave (APW) method calculation of its energy-band structure using a computational scheme derived as an extension of the work of Jepsen and Andersen[4] and Lehmann *et al.*[3] on the density-of-states problem. Using tetrahedrons as microzones with which to divide the BZ, a geometrical analysis is made of the occupied and unoccupied regions of any tetrahedron which reduces the problem of calculating $\chi(\vec{q})$ essentially to the problem of performing a volume integral over a tetrahedron with a linearized energy denominator. This procedure yields simple analytic expressions for the BZ integral which depend only on the volume of the tetrahedron and the differences of energies, $\Delta E_n(k)$, at its corners. The result is a computational scheme—not limited to constant matrix elements—which is highly accurate and, because of its simplicity, rapid to perform. For example, our results for Sc given in Sec. IV show very good agreement with the $\chi(\vec{q})$ values calculated earlier by Liu *et al.*[17]

The plan of this paper is as follows: Sec. II discusses the method and presents our analytic expressions for the $\chi(\vec{q})$ integral inside the microzone. Section III illustrates the method by means of model calculations on (i) the free-electron-gas susceptibility (i.e., the Lindhard function) and (ii) on the susceptibility of a "box" energy surface introduced by Fehlner and Loly.[9] The first model calculation tests the agreement between an analytic known result and our numerical predictions; the second tests the method to see if it can reproduce the effect of "nesting" on $\chi(\vec{q})$. Results of an *ab initio* energy-band calculation of density of states, Fermi surface, and $\chi(\vec{q})$ for Sc metal are presented in Sec. IV.

II. ANALYTIC TETRAHEDRON LINEAR ENERGY METHOD

The real part of the frequency and wave-vector-dependent spin susceptibility function in the random-phase approximation (RPA) is given by the well-known expression

$$\mathrm{Re}\chi(\vec{q},\omega)=\frac{1}{N}P\sum_{\substack{n,n'\\ \vec{k}}}\left|M^{n,n'}(\vec{k}+\vec{q}+\vec{K}_0,\vec{k})\right|^2 \times\frac{f(E_n(\vec{k}))[1-f(E_{n'}(\vec{k}+\vec{q}+\vec{K}_0))]}{E_{n'}(\vec{k}+\vec{q}+\vec{K}_0)-E_n(\vec{k})-\omega}\,, \quad (1)$$

when $E_n(\vec{k})$ is the energy of the Bloch electron at the point $\vec{k}$ of the BZ and in the band n, and $M^{nn'}$ is the oscillator-strength matrix element. At $T=0$, the Fermi function $f(E_n(\vec{k}))$ has the value 0 or 1 depending upon whether $E_n(\vec{k})$ is above or below the Fermi energy E_F. The reciprocal-lattice vector $\vec{K}_0$ keeps the point $\vec{k}+\vec{q}$ in the first Brillouin zone. In what follows we shall drop the frequency dependence from consideration as this can easily be inserted at a later point.

For purposes of discussion and a more general understanding of the problem, we should note that Eq. (1) is but a specific example of a class of so-called "spectral" (or Green's) functions. Consider for example,[1] the spectral distribution function in terms of the energylike variable ω:

$$G(\omega)=\lim_{\epsilon\to 0^+}\frac{1}{N}\sum_{\vec{k}}\frac{F(\vec{k})}{\omega-\omega(\vec{k})-i\epsilon}\,, \quad (2)$$

which has real and imaginary parts

$$\mathrm{Re}G(\omega)=P\frac{1}{N}\sum_{\vec{k}}\frac{F(\vec{k})}{\omega-\omega(\vec{k})} \quad (3)$$

and

$$\mathrm{Im}G(\omega)=\frac{\pi}{N}\sum_{\vec{k}}F(\vec{k})\delta(\omega-\omega(\vec{k}))\,. \quad (4)$$

In common practice, it is convenient to replace the summations in Eq. (3) and (4) by their integral equivalents which make it transparent that $\mathrm{Re}G(\omega)$ and $\mathrm{Im}G(\omega)$ are the Hilbert transforms of each other. Clearly, Eq. (4) has the form encountered in density-of-states calculations, whereas Eq. (3) has the form encountered in the calculation of optical (or spectral) distribution functions, the dielectric constant and of course, as stated (when the $\vec{q}$ dependence is included), the generalized susceptibility expression in Eq. (1). The method described here is thus far more applicable than to calculations of $\chi(\vec{q})$. In both Eqs. (3) and (4), integrations over the BZ (or its irreducible part) must be performed. As stated in Sec. I, there are various ways to proceed. For example, in the original method of Gilat and Raubenheimer[2] (GR) the irreducible part of the BZ is divided into cubes, at each of whose center the energy $E(\vec{k})$ and its gradient with respect to $\vec{k}$ is found. One makes the assumption that the energy varies linearly inside the cube in which case the surface of constant energy is a plane, i.e., assume the simple first term Taylor-series expansion

$$E_n(\vec{k})=E_n(\vec{k}_i)+\nabla_{\vec{k}}E_n(\vec{k})\big|_{\vec{k}=\vec{k}_i}\cdot(\vec{k}-\vec{k}_i)\,, \quad (5)$$

and $\nabla_k E_n(\vec{k})$ is the gradient at the cube center. The integral for the density of states, Eq. (4), is trans-

formed into an integral over surfaces of constant energy

$$N(E)=\frac{2\Omega}{(2\pi)^3}\int_{E(\vec{k})=E}\frac{dS}{|\nabla_{\vec{k}}E|} \tag{6}$$

(where Ω is the BZ volume) and approximated by a sum over cubes

$$N(E)\cong\frac{2\Omega}{(2\pi)^3}\sum_{n,i}\frac{S_n(E,\vec{k}_i)}{|\nabla_{\vec{k}}E_n(k_i)} \ . \tag{7}$$

The real advantage of the method lies in the fact that *analytic* expressions for the surface area inside the cube, $S_n(E,\vec{k}_i)$, are given by *GR* in terms of $E-E(\vec{k}_i)$ and $\nabla_{\vec{k}}E(\vec{k})|_{k_i}$ which allow Eq. (7) to be used for an accurate determination of $N(E)$.

Jepsen and Andersen[4] and Lehmann *et al.*[3] found that substantial simplifications can be obtained in the GR method by dividing the cubes (or rectangular and triangular prisms for the irreducible BZ wedges of the hexagonal and tetragonal crystals) into general tetrahedrons and assuming linearity for $E_n(k)$ inside each tetrahedron. $N(E)$ is still given by Eq. (7), but with the summation over tetrahedrons instead of cubes. Since the method we propose for the calculation of $\chi(\vec{q})$ is so closely related to theirs for the calculation of $N(E)$, we recast this procedure in our terms in order to provide a handy comparison between the analytic expressions obtained for both the $N(E)$ and $\chi(\vec{q})$ cases.

A. Density of states

The energy $E(\vec{k})$ is linearly expanded inside the tetrahedron, and the coefficients of expansion are determined in terms of the corner energies and coordinates as was done in the work of Lehmann and Taut[3] and Jepsen and Andersen.[4] For this purpose it is convenient to arrange the energy at the corners of the tetrahedrons in increasing or decreasing order. Let $\vec{k}_i$ $(i=1, 2, 3, 4)$ be the coordinates of the four corners of the tetrahedron. Denoting $E_n(\vec{k}_i)$ by E_i for $i=1, 2, 3, 4$, we assume

$$E_4\le E_3\le E_2\le E_1. \tag{8}$$

We further assume a linear expansion for the energy $E(\vec{k})$ inside the tetrahedron:

$$E(\vec{k})=E(\vec{k}_4)+\vec{b}\cdot(\vec{k}-\vec{k}_4)\ , \tag{9}$$

where

$$\vec{b}=\sum_{i=1}^{3}[E(\vec{k}_i)-E(\vec{k}_4)]\,\vec{r}_i \tag{10}$$

and

$$\vec{r}_i\cdot\vec{k}'_j=\delta_{ij}$$

with

$$\vec{k}'_j=\vec{k}_j-\vec{k}_4\ ;\quad j=1, 2, 3\ . \tag{11}$$

Writing

$$\vec{r}_1=\vec{k}'_2\times\vec{k}'_3/v\ ;\quad \vec{r}_2=\vec{k}'_3\times\vec{k}'_1/v\ ;\quad \vec{r}_3=\vec{k}'_1\times\vec{k}'_2/v\ , \tag{12}$$

where $v=\vec{k}'_1\cdot(\vec{k}'_2\times\vec{k}'_3)=6$ times the volume of the tetrahedron, then in this notation [and using Eq. (7)] the contribution to the density of states from the ith tetrahedron corresponding to the nth band is given by

$$N_{n,i}(E)=\frac{2\Omega}{(2\pi)^3}\,\frac{dS(E)}{|\vec{b}|}\ . \tag{13}$$

From considerations of the general geometric properties of the cross-sectional area of a plane intersecting a polyhedron, analytical expressions for $dS(E)/|\vec{b}|$ have been given by Jepsen and Andersen and Lehmann and Taut. If we write out these expressions in terms of our definitions, we have

$$dS(E)=\begin{cases} f_0, & E_4\le E\le E_3 \\ f_0-f_1, & E_3\le E\le E_2 \\ f_3, & E_2\le E\le E_1 \\ 0\ , & E\le E_4 \ \text{ and } \ E_1\le E\ , \end{cases} \tag{14}$$

where

$$\begin{aligned} f_0|\vec{b}|^{-1}&=\frac{v}{2}\,\frac{(E-E_4)^2}{(E_3-E_4)(E_2-E_4)(E_1-E_4)}\ , \\ f_1|\vec{b}|^{-1}&=\frac{v}{2}\,\frac{(E-E_3)^2}{(E_3-E_4)(E_2-E_3)(E_1-E_3)}\ , \\ f_3|\vec{b}|^{-1}&=\frac{v}{2}\,\frac{(E-E_1)^2}{(E_1-E_4)(E_1-E_3)(E_1-E_2)}\ . \end{aligned} \tag{15}$$

As is clear from these simple analytic expressions, energy gradients do not occur explicitly in this formalism (as they do in the GR scheme) and so none of the disadvantages of the gradient schemes occur here. The method is simple to implement

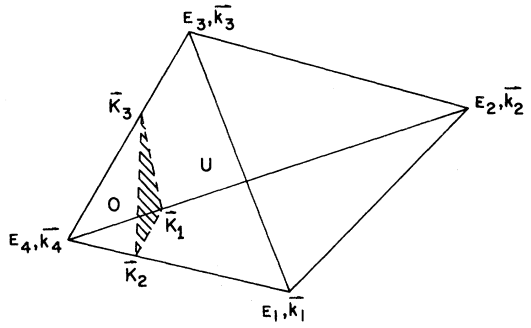

FIG. 1. Intersection of the Fermi surface (plane) with the tetrahedron for the case $E_4<E_F<E_3<E_2<E_1$. The occupied region of the tetrahedron (denoted by O) is also a tetrahedron: $(\vec{k}_4, \vec{K}_1, \vec{K}_2, \vec{K}_3)$. The unoccupied region (U) is a sum of three tetrahedrons.

and results in rapid and accurate computations of the density of states of real metals.

B. Generalized susceptibility $\chi(\vec{q})$

As in the case of the density-of-states calculation, our purpose is to develop a suitable analytic integration scheme for the Brillouin-zone integration of Eq. (1) taking into account the principal-value nature of the integral. As in Sec. IIA, the scheme proceeds by dividing the entire Brillouin zone (or the irreducible part of it) into nonoverlapping tetrahedra. Although it is not necessary, we assume that all tetrahedra are of the same size, as this saves a certain amount of computational effort. Since we make a linear approximation to the energy bands inside each tetrahedron, the surfaces of constant energy are again planes. Now, the fractional volume of a given tetrahedron that contributes to the susceptibility function is determined by the intersection of constant energy surfaces (planes) corresponding to $E_n(\vec{k})$ and $E_{n'}(\vec{k}+\vec{q})$. Inside this fractional volume of the tetrahedron the product of $f(E_n(\vec{k}))\times[1-f(E_{n'}(\vec{k}+\vec{q}))]$ must have the value unity. As we shall see, this fractional volume is either a tetrahedron or a sum of (at most, nine) tetrahedrons. Thus, after taking care of the Fermi factors it is then only necessary to be able to perform a volume integration over a tetrahedron with a linearized energy denominator. As we shall see this integral is easily done.

Let us begin by determining the fractional volume a given tetrahedron that contributes to the integral. As before, it is convenient to arrange the energy in the order given by Eq. (8). [We ignore here the possibility that two or more corner energies may be identical in order to keep the discussion simple as these cases can be easily incorporated in the results.] The energy at a point $\vec{k}$ can be determined in the linear approximation from Eqs. (9)–(12). To determine the occupied volume of the tetrahedron corresponding to $f(E_n(\vec{k}))=1$ one has to consider the following cases:

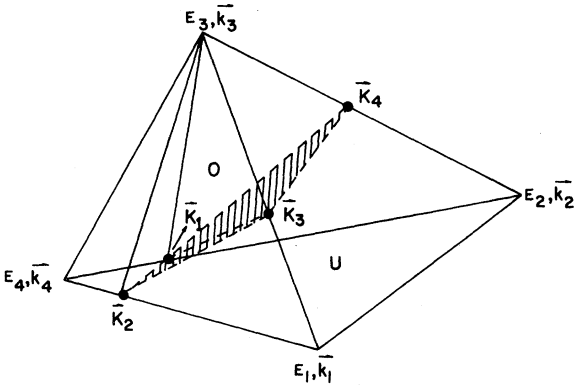

FIG. 2. Intersection of the Fermi surface with the tetrahedron for the case $E_4<E_3<E_F<E_2<E_1$. The occupied region (O) is a sum of three tetrahedrons: ($\vec{k}_4$, $\vec{k}_3$, $\vec{K}_1$, $\vec{K}_2$), ($\vec{k}_3$, $\vec{K}_2$, $\vec{K}_3$, $\vec{K}_1$), ($\vec{k}_3$, $\vec{K}_1$, $\vec{K}_3$, $\vec{K}_4$). The unoccupied region (U) is also a sum of three tetrahedrons.

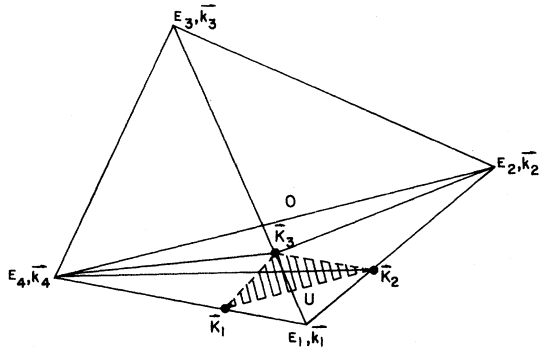

FIG. 3. Intersection of the Fermi surface with the tetrahedron for the case $E_4<E_3<E_2<E_F<E_1$. The occupied region of the tetrahedron (O) is a sum of three tetrahedrons: ($\vec{k}_3$, $\vec{k}_4$, $\vec{K}_3$ $\vec{k}_2$), ($\vec{k}_4$, $\vec{K}_1$, $\vec{K}_2$, $\vec{K}_3$), ($\vec{k}_4$, $\vec{k}_2$, $\vec{K}_2$, $\vec{K}_3$). The unoccupied region is a tetrahedron.

(i) $E_F \leq E_4<E_3<E_2<E_1$. In this case the entire tetrahedron is unoccupied and this tetrahedron does not contribute to the integral.

(ii) $E_4<E_F<E_3<E_2<E_1$. The Fermi surface is a plane inside the tetrahedron and intersects the sides of the tetrahedron at the points $\vec{K}_1$, $\vec{K}_2$, $\vec{K}_3$ (cf. Fig. 1). This plane separates the occupied region (labeled O) from the unoccupied region (U). As is seen the occupied region is *another* tetrahedron. The unoccupied portion may be constructed as a sum of three tetrahedrons.

(iii) $E_4<E_3<E_F<E_2<E_1$. In this case, the Fermi surface intersects the sides of the tetrahedron at points $\vec{K}_1$, $\vec{K}_2$, $\vec{K}_3$, $\vec{K}_4$. As shown in Fig. 2 the occupied portion of the tetrahedron (O) is a sum of three tetrahedrons: ($\vec{k}_4$, $\vec{k}_3$, $\vec{K}_1$, $\vec{K}_2$); ($\vec{k}_3$, $\vec{k}_1$, $\vec{K}_2$, $\vec{K}_3$); ($\vec{k}_3$, $\vec{K}_1$, $\vec{K}_3$, $\vec{K}_4$). The unoccupied portion (U) is also a sum of three tetrahedrons (not shown).

(iv) $E_4<E_3<E_2<E_F<E_1$. The Fermi surface intersects the sides at points $\vec{K}_1$, $\vec{K}_2$, $\vec{K}_3$. As shown in Fig. 3 the occupied portion of the tetrahedron is a sum of three tetrahedrons: ($\vec{k}_4$, $\vec{k}_3$, $\vec{k}_2$, $\vec{K}_3$); ($\vec{k}_4$, $\vec{K}_3$, $\vec{K}_2$, $\vec{K}_1$); ($\vec{k}_4$, $\vec{K}_2$, $\vec{K}_3$, $\vec{k}_2$). The unoccupied portion is a single tetrahedron ($\vec{K}_3$, $\vec{K}_1$, $\vec{k}_2$, $\vec{K}_2$).

(v) $E_4<E_3<E_2<E_1\leq E_F$. The entire tetrahedron is occupied.

Given the occupied volume corresponding to $f(E_n(\vec{k}))$ which is a tetrahedron or a sum of three tetrahedrons, it is then necessary to determine from the above volume the region over which $f(E_{n'}(\vec{k}+\vec{q}))$ is unoccupied. As seen from all cases (i)–(iv), the unoccupied portion of a tetrahedron is

either a tetrahedron or the sum of three tetrahedrons. Thus we see that the fractional volume of a given tetrahedron which contributes $[f(1-f)=1]$ to the susceptibility function is either a tetrahedron or a sum of tetrahedrons. It is now necessary to perform a volume integral over a tetrahedron with a linearized energy denominator. It should be mentioned that a slightly different and simpler approach to the determination of the occupied volume of a given tetrahedron was discussed by Lehmann and Taut[3] based on the use of $[f(E_n(\vec{k}))-f(E_{n'}(\vec{k}+\vec{q}))]$ in Eq. (1) for $\chi(\vec{q})$. This also results in their occupied and unoccupied volumes being written, in some cases (e.g., cf. our Fig. 3) as the difference of two tetrahedrons rather than our sum of three tetrahedrons. While our choice thus complicates the geometrical considerations, we prefer the possible greater numerical accuracy which may result from the fact that our integrals are always positive, unlike the case of Lehmann and Taut.

Assuming the matrix elements to be constant inside the tetrahedron, we have to perform the following integral

$$I_{nn'}(\vec{q})=\int_{\text{tetra}}\frac{d^3k}{E_{n'}(\vec{k}+\vec{q})-E_n(\vec{k})}\ . \tag{16}$$

Using a linearized energy denominator we have (see the Appendix)

$$I_{nn'}=3\Omega\left(\frac{V_1^2}{D_1}\ln\left|\frac{V_1}{V_4}\right|+\frac{V_2^2}{D_2}\ln\left|\frac{V_2}{V_4}\right|+\frac{V_3^2}{D_3}\ln\left|\frac{V_3}{V_4}\right|\right), \tag{17}$$

where Ω is the volume of the tetrahedron,

$$D_1=(V_1-V_4)(V_1-V_3)(V_1-V_2)\ ,$$

$$D_3=(V_3-V_4)(V_3-V_2)(V_3-V_1)\ ,$$

$$D_2=(V_2-V_4)(V_2-V_3)(V_2-V_1)\ , \tag{18}$$

and

$$V_i=E_{n'}(\vec{k}_i+\vec{q})-E_n(\vec{k}_i);\ i=1,2,3,4\ .$$

Thus we see that the contribution to the susceptibility from a given tetrahedron is determined solely from a knowledge of the energy-band eigenvalues at the corners of the tetrahedron. One does not have to calculate the gradient of the energy in this method.

As a final step, one must carefully obtain the limit of the Eq. (17) for the case when some of the V_i's are zero or equal.

(i) $V_1=V_2=V_3=V_4=V\neq 0$,

$$I=\Omega/V\ .$$

(When $V=0$, we neglect the contribution from that particular tetrahedron.)

(ii) $V_1=V_2=V_3=V\neq V_4,\ V\neq 0$,

$$I=3\Omega\left(\frac{V_4^2}{(V-V_4)^3}\ln\left|\frac{V}{V_4}\right|+\frac{\frac{3}{2}V_4^2+\frac{1}{2}V^2-2VV_4}{(V-V_4)^3}\right)\ . \tag{19}$$

(When $V=0$, we neglect the contribution from such a tetrahedron.)

(iii) $V_1=V_2=V,\ V_3=V_4=V'$

$$I=3\Omega\left(\frac{2VV'}{(V-V')^3}\ln\left|\frac{V'}{V}\right|+\frac{V+V'}{(V-V')^2}\right)\ . \tag{20}$$

(iv) $V_1=V_2=V\neq V_3\neq V_4$

$$I=3\Omega\left(\frac{V_3^2}{(V_3-V)^2(V_3-V_4)}\ln\left|\frac{V_3}{V}\right|+\frac{V_4^2}{(V_4-V)^2(V_4-V_3)}\ln\left|\frac{V_4}{V}\right|+\frac{V}{(V_3-V)(V_4-V)}\right). \tag{21}$$

At this stage we must consider how to include the matrix elements in our integration scheme. Although a large number of calculations have been performed assuming constant matrix elements,[15] recent calculations[16,18] have shown that matrix elements play a very important role in determining the location and magnitude of structures in $\chi(\vec{q},\ 0)$. The inclusion of matrix elements in our scheme is simply done by calculating the matrix elements at the center of each tetrahedron and assuming it to be constant throughout the tetrahedron. This perhaps is not too bad an approximation if the tetrahedrons are small enough. The advantage of using the tetrahedrons as microzones is clear from our discussion. By linearly interpolating the energy denominator with respect to corners of the tetrahedrons, as was done in Lehmann and Taut, the knowledge of energy gradients is not required. We have demonstrated that the appropriate volume of the microzone which contributes to the integral is either a tetrahedron or sum of tetrahedrons. This conclusion was drawn from the observation that a constant energy surface can intersect a tetrahedron in only three distinct ways. In the present scheme, the volume integral is performed directly, which eliminates a lot of tedious considerations associated with the case when $f(E_{n'}(\vec{k}+\vec{q}))-f(E_n(\vec{k}))$ is not constant inside the microzone. In the work of Lipton and Jacobs,[5] where cubes were taken as the microzones (and the integration scheme was different from ours), the case when $f(E_{n'}(\vec{k}+\vec{q}))-f(E_n(\vec{k}))$ is not constant inside the cube poses many computational problems, because one has to take into consideration the various types of contributions to the susceptibility arising from the various different ways the Fermi surface can cut a given cube. The simplicity of the way in which Fermi factors can be taken into account in the present scheme and the analytical expres-

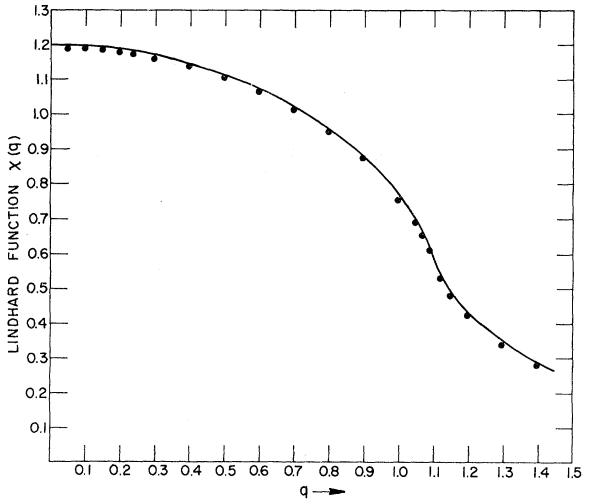

FIG. 4. Comparison of the numerical (●) and analytical results (solid line) for the free-electron-gas susceptibility (Lindhard function). The calculations were performed for a simple cubic reciprocal lattice with Fermi radius lattice $k_F = 0.55$ with Γ-$X = 1$. The mesh size for the above numerical calculation was 12 divisions along Γ-X.

sions for the volume integral make the computational aspects especially simple.

III. CALCULATIONS OF $\chi(\vec{q})$ FOR SOME MODEL SYSTEMS

As with any new method, it is important to determine its computational feasibility and the accuracy with which it can predict observable physical quantities. We here apply this method to two severe test cases, namely, model systems for which the results are known or which have a special physical feature such as a "nesting" Fermi surface.

In our first model calculation we determine the static susceptibility function $\chi(\vec{q})$ for a free-electron gas. The analytical form of $\chi(\vec{q})$ for a free-electron gas (known as the Lindhard function) is well known, and thus we can compare our numerical results with the analytical result. The reciprocal lattice chosen was simple cubic and the result shown in the diagram corresponds to a mesh size of 12 divisions along Γ-X. The Fermi wave vector k_F was chosen to be 0.55 (Γ-$X = 1$). As can be seen from Fig. 4 there is excellent agreement between the numerical and analytical results. The numerical results differ from the analytical results mostly around $q \sim 2k_F$, where there is a logarithmic singularity in the slope of the Lindhard function. The maximum deviation from the analytical value was never more than 2.5% and the average deviation was estimated to be around 1.25%. The accuracy can be improved substantially by choosing a denser mesh than was the case for the results shown here. The calculation was repeated with 16 divisions along Γ-X to check the convergence property of our numerical procedure. The maximum deviation, which again occurred around $q = 2k_F$, was less than 1.5%, and the average deviation for the entire curve was around 0.75%. Furthermore, the deviation from the exact value was systematic in nature rather than random, with all points calculated lying below the analytic value.

The other model structure for which a susceptibility function was computed was introduced by

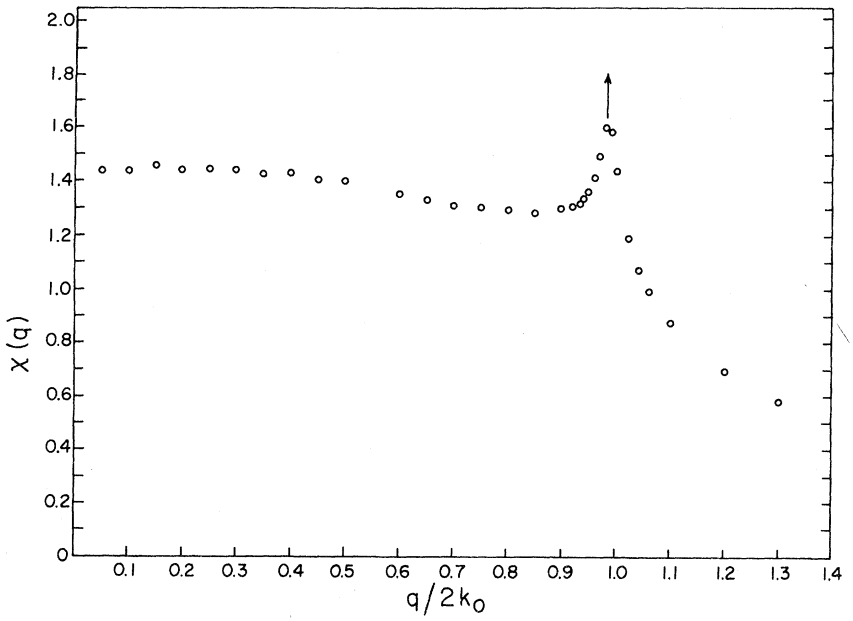

FIG. 5. Results of a numerical calculation of the susceptibility function corresponding to the energy dispersion given by Eq. (23) in the text. The calculation was performed for a simple cubic lattice, with parameters $k_0 = 0.5$ and $R = 8$ with Γ-$X = 1$, and a mesh of 12.

Fehlner and Lolly.[9] The energy dispersion in this case is given by

$$\epsilon(\vec{k}) = [k^2 + 2R \max(|k_x|, |k_y|, k_z|)]/(1+R), \quad (22)$$

where R is a certain parameter such that when $R = 0$, one has the energy dispersion formula for the free-electron gas problem where the surfaces of constant energy are spheres. When $R \to \infty$, the surfaces of constant energy are cubes as was first considered by Evenson and Liu.[15] The purpose of calculating the $\chi(\vec{q})$ for a "box" energy surface was to test if the procedure can reproduce the effect of "nesting" features in $\chi(\vec{q})$. As has been emphasized in the literature, flat pieces of Fermi surface which can be joined by a constant wave vector give rise to maxima in the susceptibility function. The susceptibility function $\chi(\vec{q})$ for a cube has a logarithmic singularity at $q = 2k_0$, where k_0 is the maximum extension of the Fermi surface in the x direction. The $\chi(\vec{q})$ calculated with the energy dispersion formula of Fehlner and Loly (with $R = 8$, $k_0 = 0.5$) shows a sharp peak which occurs at a value of q somewhat less than $2k_0$. Our results for q along Γ-X are shown in Fig. 5.

IV. $\chi(\vec{q})$ for scandium metal

Interest in the electronic structure of Sc metal is high because of its unusual properties as a light transition metal and because many of its physical properties resemble those of the heavy rare-earth metals which also have the hcp structure. Although not magnetic like the rare-earths, knowledge about the $\chi(\vec{q})$ of Sc can be instructive about the magnetic structures of its alloys with magnetic rare-earths. The peaks in $\chi(\vec{q})$ are important because of the role they play in determining Kohn type anomalies in the phonon spectra.[15]

The electronic energy band structure was determined using the augmented-plane-wave (APW) method. The warped muffin-tin crystal potential was derived in the usual manner[20] as a superposition of Hartree-Fock-Slater neutral atomic charge densities, but for the configuration $3d^2 4s^1$ of Sc. Exchange was treated in the Slater $\rho^{1/3}$ approximation with the exchange parameter $\alpha = 1$. Unlike the case of earlier calculations,[21,22] we used the low-temperature x-ray values of the lattice constants determined recently by Mueller,[23] i.e., $a = 6.2391$ and $c = 9.9316$. The computed band structure was found to be in agreement with the earlier nonrelativistic results of Fleming and Loucks[21] and the relativistic results of Das *et al.*,[22] but with some small differences arising from the different atomic configuration and/or lattice constants used.

The calculated energy eigenvalues were then fitted with a Fourier series; the root-mean-square error in the fitted energy at 60 $\vec{k}$ points calculated by the APW scheme for the first four bands was less than 3 mRy. The electronic density of states $N(E)$ and Fermi energy were calculated using the linear interpolation of energy inside the tetrahedrons, as described in Sec. III. Finally, the Fermi surface (FS) was constructed in the usual manner; cross sections are shown in Fig. 6 for some of the principal planes of the double-Brillouin-zone representation. As expected, this FS is also very similar to those found in earlier calculations.[21,22]

Using the analytic tetrahedron linear energy method described in Sec. III, we have calculated $\chi(\vec{q})$, in the constant matrix element approximation for $\vec{q}$ along the Γ-A direction (the c direction). In the actual computations we used 45 distinct points in the hexagonal plane and 9 such planes to construct the tetrahedrons—making in all 1536 tetrahedrons in $\frac{1}{24}$th of the irreducible Brillouin zone. Only the 3rd and 4th bands were included in computing $\chi(\vec{q})$ since these two bands, which intersect the Fermi energy in scandium, determine the structure in the susceptibility function. The values of $E(\vec{k})$ and $E(\vec{k}+\vec{q})$ for these bands were obtained at corners of the tetrahedrons using the Fourier series fit program mentioned earlier. If $\vec{k}$ lies in some tetrahedron in the irreducible Brillouin zone (IBZ), then $\vec{k}+\vec{q}$ in the most general case must be translated through a reciprocal lattice vector and rotated to bring it back to the IBZ. If the $\vec{k}$ integration is carried out only over the irreducible part of the BZ, then a sum must be performed over all wave vectors in the star of $\vec{q}$ in order to obtain $\chi(\vec{q})$. In the present case the choice

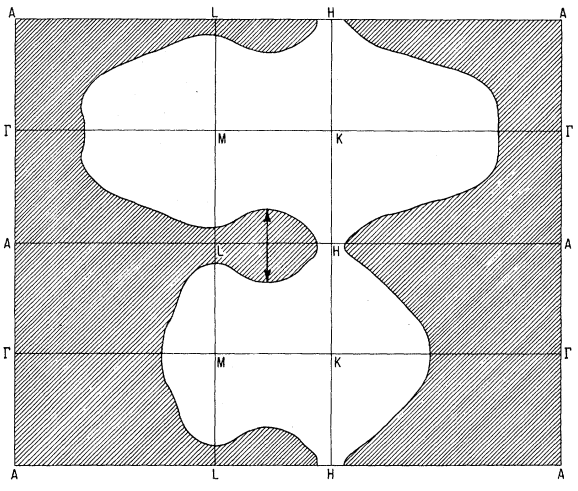

FIG. 6. Intersections of the scandium Fermi surface with the symmetry planes of the Brillouin zone in the double zone representation. Cross-hatched areas are holes. The magnitude of the indicated wave vector $\vec{Q}$ corresponds roughly to the position where the first maxima of $\chi(\vec{q})$ occurs.

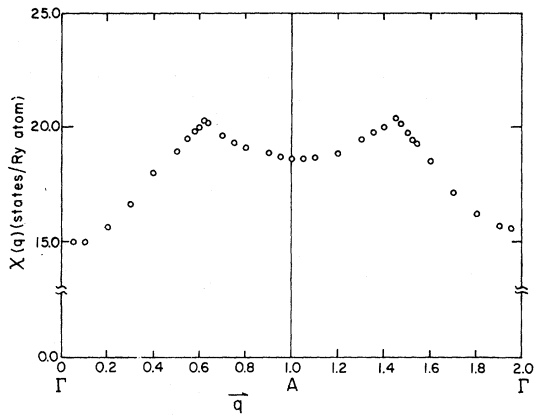

FIG. 7. Susceptibility function $\chi(\vec{q})$ for scandium along the Γ-A-Γ direction. The calculation was performed with 1536 tetrahedrons in $\frac{1}{24}$th of the Brillouin zone. The two peaks in the curve occur at positions $(0, 0, 0.31)2\pi/c$, $(0, 0, 0.72)2\pi/c$. The $\vec{q} \to 0$ limit of the function $\chi(\vec{q})$ agrees to within 1% with $\frac{1}{2}$ times the density of states at E_F (obtained by an independent calculation).

of $\vec{q}$ along the c direction made the situation simpler to handle. Since the integration was carried out in $\frac{1}{24}$th of the BZ, the contributions corresponding to vectors $(0, 0, q)$ and $(0, 0, -q)$ were calculated and added to obtain $\chi(\vec{q})$.

A plot of $\chi(q)$ vs q along Γ-A is shown in Fig. 7 and is similar to that shown by Liu *et al.*[14] However, we find *two* peaks in the curve situated at $\vec{q} = (0, 0, 0, 31)2\pi/c$ and $\vec{q} = (0, 0, 0.72)2\pi/c$ rather than the *three* broad peaks shown by Liu *et al.*[14] from the calculation of Wakabayashi[24] at approximately $\vec{q} = (0, 0, 0.35)2\pi/c$, $(0, 0, 0.57)2\pi/c$, and $(0, 0, 0.77) \times 2\pi/c$. We also do not find the structure (oscillations) shown in the first and (especially) the third peak of Wakabayashi,[24] but these small differences may be entirely due to the small differences between our respective Fermi surfaces. It is gratifying to note that the first peak in $\chi(\vec{q})$ in Fig. 7 corresponds very closely to the experimental value of the magnetic wave vector $\vec{q}_m = (0, 0, 0.28)2\pi/c$ found for the dilute alloys of Sc with rare earths.[25-27]

What may be said about the phonon dispersion curves and their relation to $\chi(\vec{q})$? It is generally believed that the kinks in the phonon curves arise from peaks in $\chi(\vec{q})$. The argument for this goes as follows. The diagonal element of the dielectric function $\epsilon(\vec{q}, \vec{q})$ is related to $\chi(\vec{q})$ through the relation

$$\epsilon(\vec{q}, \vec{q}) = 1 + Av(\vec{q})\chi(\vec{q}) ,$$

where A is a constant and $v(\vec{q})$ is the transform of the electrostatic electron-electron interaction including exchange and correlation effects. Since the dielectric screening by the conduction electrons plays an important role in determining the ion-ion interaction transmitted by the conduction electrons, one might expect a sharp maximum in $\chi(\vec{q})$ to manifest itself also as an anomaly in the phonon dispersion curve. For Sc metal, Wakabayashi *et al.*[24] have observed a kink in the longitudinal acoustic (LA) branch at a wave vector $\vec{q} = (0, 0, 0.27)2\pi/c$. This $\vec{q}$ value is close to the observed magnetic wave vector $\vec{q}_m$ and close to our first peak in $\chi(\vec{q})$. Wakabayashi *et al.*[24] could find no other kinks which would correspond to the other peaks(s) in the theoretical $\chi(\vec{q})$ curves.

Finally, as noted by Liu *et al.*,[17] although yttrium metal has a very similar electronic structure, and shows similar peaks in the theoretical[17] $\chi(\vec{q})$ to those found for Sc, no phonon anomalies were found by Sinha *et al.*[28] near the first peak in $\chi(\vec{q})$. Instead, two sharp dips in the longitudinal optic (LO) branch at $(0, 0, 0.625)2\pi/c$ and $(0, 0, 0.775)2\pi/c$ were observed. In view of the similarities in the electronic structures of Sc and Y, one expected the Kohn anomalies in both the metals to be observed roughly at the same positions. Even though the susceptibility matrix plays a very complex role in the dynamical matrix for phonon spectra it is possible that the $\chi(\vec{q})$, including matrix elements, using accurate solid-state wave functions will help in resolving this question. Such calculations have become increasingly important since it is now widely recognized that the matrix elements do play an important role in determining the peaks and the general structure. Calculations are now underway[29] for both Sc and Y which utilize the methods developed here with APW wave functions for the calculation of matrix elements.

ACKNOWLEDGMENTS

We are greatly indebted to F. M. Mueller for close collaboration during the early phases of this work, for valuable suggestions, and for constant encouragement, to R. P. Gupta for critical comments, helpful advice and valuable interactions, and to D. D. Koelling and B. N. Harmon for stimulating discussions and helpful references to the literature. We are grateful to Sue Katilavas for computational assistance.

APPENDIX

The calculation of the volume integral over a tetrahedron with a linearized energy denominator is straightforward. The integral to be evaluated is

$$I_{n,n'}(\vec{q}) = \int_{\text{tetra}} \frac{d^3k}{E_{n'}(\vec{k}+\vec{q}) - E_n(\vec{k})} . \qquad \text{(A1)}$$

Let the coordinates of the corners of the tetrahe-

dron be $\vec{k}_1$, $\vec{k}_2$, $\vec{k}_3$, $\vec{k}_4$, and define

$$V_i = E_{n'}(\vec{k}_i + \vec{q}) - E_n(\vec{k}_i) \ . \tag{A2}$$

For convenience, let us choose a coordinate system such that

$$\vec{k}_1 = (0, 0, 0) \ , \qquad \vec{k}_2 = (X_1, 0, 0) \ ,$$

$$\vec{k}_3 = (X_2, Y_2, 0) \ , \qquad \vec{k}_4 = (X_3, Y_3, Z_3) \ , \tag{A3}$$

and expand the energy difference linearly inside the tetrahedron:

$$E_{n'}(\vec{k}+\vec{q}) - E_n(\vec{k}) = A + BX + Cy + Dz \ . \tag{A4}$$

The coefficients A, B, C, D are determined from the value of the energy differences at the corners of the tetrahedron. Thus,

$$A = V_1 , \quad A + BX_1 = V_2 , \quad A + BX_2 + CY_2 = V_3 ,$$

$$A + BX_3 + CY_3 + DZ_3 = V_4 \ . \tag{A5}$$

With this coordinate system the volume integral over the tetrahedron can be written as

$$I = \int_0^{Z_3} dz \left[\int_{\alpha z+\beta}^{mz+n} dx \int_{tz}^{pz+qx+r} dy \, \frac{1}{A + Bx + Cy + Dz} \right.$$

$$\left. - \int_{\alpha' z+\beta'}^{m'z+n'} dx \int_{t'z}^{p'z+q'x+r'} dy \, \frac{1}{A + Bx + Cy + Dz} \right], \tag{A6}$$

where $(\alpha, \beta, m, n, p, q, r, t)$ and $(\alpha', \beta', m', n', p', q', r', t')$ are related to the coordinates of the corners of the tetrahedron. The final result of the integration depends only on V_1, V_2, V_3, V_4 and the volume of the tetrahedron, as expected.

Note added in proof. We have been informed by P. A. Lindgård that he has independently derived the same analytic expressions for $I_{n,n'}(\vec{q})$ given in this paper.

---

†Supported by the National Science Foundation, the Air Force Office of Scientific Research and the U. S. Atomic Energy Commission.

[1]The review by G. Gilat [J. Comp. Phys. 10, 432 (1972)] contains a comparison of methods and extensive references.

[2]G. Gilat and L. J. Raubenheimer, Phys. Rev. 144, 390 (1966).

[3]G. Lehmann, P. Rennert, M. Taut, and H. Wonn, Phys. Status Solidi 37, K27 (1970); G. Lehmann and M. Taut, *ibid.* 54, 469 (1972).

[4]O. Jepsen and O. K. Andersen, Solid State Comm. 9, 1763 (1971). See also the recent extension of the tetrahedron method by P. A. Lingård [Risø-M-1701, Library of the Danish AEC and Lectures at the XI Annual Winter School for Theoretical Physics, Poland, 1974 (unpublished)].

[5]D. Lipton and R. L. Jacobs, J. Phys. C 3, 1388 (1970).

[6]D. Lipton, J. Phys. F 1, 469 (1971).

[7]F. M. Mueller, J. W. Garland, M. H. Cohen, and K. H. Bennemann, Ann. Phys. (N.Y.) 67, 19 (1971).

[8]J. B. Diamond, J. Appl. Phys. 42, 1543 (1971).

[9]W. R. Fehlner and P. D. Lolly, Solid State Commun. 14, 653 (1974).

[10]M. Blackman, Proc. R. Soc. A 159, 416 (1937).

[11]G. Gilat and G. Dolling, Phys. Lett. 8, 304 (1964).

[12]J. F. Cooke and R. F. Wood, Phys. Rev. B 5, 1276 (1972).

[13]R. Kubo, J. Phys. Soc. Jpn. 12, 570 (1957).

[14]R. E. Peierls, *Quantum Theory of Solids* (Clarendon, Oxford, 1955).

[15]W. E. Evenson and S. H. Liu, Phys. Rev. 178, 783 (1969).

[16]R. P. Gupta and S. K. Sinha, Phys. Rev. B 3, 2401 (1971).

[17]S. Liu, R. P. Gupta, and S. K. Sinha, Phys. Rev. B 4, 1100 (1971).

[18]J. F. Cooke, H. L. Davis, and M. Mostoller, Phys. Rev. B 9, 2485 (1974).

[19]J. F. Janak, Phys. Lett. A 28, 570 (1969); J. F. Janak, D. E. Eastman, and A. R. Williams, Solid State Commun. 8, 271 (1970).

[20]See L. F. Matthiess, Phys. Rev. 139, A1893 (1965) for the superposition of charge method, and D. D. Koelling, A. J. Freeman, and F. M. Mueller, Phys. Rev. 31, 1318 (1970).

[21]G. S. Fleming and T. L. Loucks, Phys. Rev. 173, 685 (1968).

[22]S. G. Das, A. J. Freeman, D. D. Koelling, and F. M. Mueller, AIP Conf. Proc. 10, 1304 (1973).

[23]M. Mueller (unpublished).

[24]The plot of $\chi(q)$ for Sc, shown by Liu *et al.* (Ref. 17) is taken from N. Wakabayashi [Ph. D. thesis (Iowa State University, Ames, Iowa, 1969) (unpublished)]. The observed phonon spectra are reported by N. Wakabayashi, S. K. Sinha, and F. H. Spedding, Phys. Rev. B 4, 2398 (1971).

[25]H. R. Child and W. C. Koehler, J. Appl. Phys. 37, 1353 (1966).

[26]H. R. Child and W. C. Koehler, Phys. Rev. 174, 562 (1968).

[27]W. C. Koehler, H. R. Child, E. O. Wollan, J. W. Cable, J. Appl. Phys. 34, 1335 (1963).

[28]S. K. Sinha, T. O. Brun, L. D. Muhlstein, and J. Sakurai, Phys. Rev. B 1, 2430 (1970).

[29]R. P. Gupta, J. Rath, and A. J. Freeman (unpublished).